Synchrophasor Estimation for Three Phase Systems Based on Taylor Extended Kalman Filtering

Roberto Ferrero, *Senior Member, IEEE*, Paolo Attilio Pegoraro, *Senior Member, IEEE*, Sergio Toscani, *Senior Member, IEEE*

***Abstract*— Synchronized phasor and frequency measurements are key tools for the monitoring and management of modern power systems. Under dynamic conditions, it is vital to define algorithms that allow accurately measuring time-varying signals with short latencies and high reporting rates. A dynamic phasor model can help the design of these algorithms and, in particular, of those based on the Kalman filter approach.**

This paper proposes a three-phase synchrophasor estimator based on the Extended Kalman filter; state variables are obtained from Taylor expansions of amplitudes and phase angles. The underlying dynamic model takes into account the inherent relationship among the phases and includes harmonics in a effective way. The process noise covariance matrix that allows representing the uncertainty introduced by the dynamic model has been written by considering that practical ac power systems are nearly three-phase symmetric during typical operation. This *a priori* information allows improving noise rejection and increasing accuracy in presence of amplitude modulation, as highlighted by the reported simulation results.

***Index Terms*—Phasor Measurement Unit, Synchrophasor estimation, Frequency, Kalman Filter, Harmonics, Three-phase systems.**

I. Introduction

Synchronized measurement of electrical signal parameters, namely amplitude, phase angle, frequency and rate of change of frequency (ROCOF), represents a very important topic in power grids since Phasor Measurement Units (PMUs) were introduced. PMUs rely on a coordinated universal time (UTC) reference to accurately define the measurement instant and thus associating a timestamp with each measured quantity [1] (hence the name synchophasor). The PMUs and their typical reporting rates were originally designed to deal with the usual dynamics of transmission networks; however PMUs are expected to play a major role also in the wide area monitoring of distribution systems.

Time-varying parameters can be accurately measured only if specifically designed techniques are implemented. The combination of rapidly evolving signals and UTC-referenced timebase have led to the need for PMU algorithms that are tailored for highly dynamic conditions, thus relying on dynamic estimation models.

The relevance of time-varying conditions is highlighted by the synchrophasor standard IEEE C37.118 and even more by the most recent revisions IEEE C37.118.1-2011 [2] and IEEE C37.118.1a-2014 [3] (superseded by the new joint IEC-IEEE standard 60255-118-1 [4]), which introduced the definition of dynamic synchrophasor, and prescribed also dynamic tests (e.g. in the presence of amplitude and phase modulation or frequency ramp) for compliance testing of commercial PMUs.

For these reasons, the literature on dynamic synchrophasor, frequency and ROCOF measurements is growing in recent years and many different techniques have been applied. In [5], a dynamic phasor model (Taylor-Fourier, TF, model) based on a Taylor expansion of the phasor around the measurement instant is proposed; the same approach has been adopted by [6]. In [7], [8] discrete Fourier transform (DFT) corrections based on a TF model are considered. IpDFT has also been successfully applied to follow frequency variations in the presence of disturbances [9] and it has been extended by using a Taylor series-based model of the synchrophasor [10]. In [11] the model in [5] is considered to design a two-channel PMU algorithm that can simultaneously comply with standard requirements for protection and measurement applications, by promptly reacting to fast changes in the input signal. In [12] the Taylor expansion of magnitude and phase angle of the Space Vector (SV) signal is used to estimate the positive sequence synchrophasor and frequency in three-phase systems, while in [13] the SV transformation is exploited jointly with the TF model. In [14], the dynamic model is adaptively updated to include other frequency components and improve the synchrophasor estimation via compressive sensing.

The Kalman filter is often used to perform DFT-like filtering [15], but it can be extended to include the TF paradigm [16] resulting in a Taylor-Kalman filter (TKF) for dynamic synchrophasor tracking. In [17] the TKF is modified to improve the model of phasor derivatives and phase angle dynamics. In [18] a smoothed TKF with enhanced frequency estimation under off-nominal conditions is presented.

In the above formulations, only the fundamental frequency component is considered. However, harmonics can be harmful for dynamic phasor estimation and they directly affect TKF-based measurements. For these reasons, [19] proposes to include harmonics in the state-space and in [20] the modified TKF is extended and improved to estimate both fundamental

R. Ferrero is with the Department of Electrical Engineering and Electronics, University of Liverpool, Liverpool, UK (email: roberto.ferrero@liverpool.ac.uk).

P. A. Pegoraro is with the Department of Electrical and Electronic Engineering of the University of Cagliari, Piazza d'Armi, 09123 Cagliari, Italy (email: paolo.pegoraro@unica.it).

S. Toscani is with the Dipartimento di Elettronica, Informazione e Bioingegneria, Politecnico di Milano, Milan, Italy (email: sergio.toscani@polimi.it).

 DOI:10.1109/TIM.2020.2983622
Publisher version:https://ieeexplore.ieee.org/document/9047878

and harmonic synchrophasors under dynamic conditions.

All of these algorithms use a linear formulation of the TKF based on the Taylor expansion of the phasors, thus introducing complex derivatives that blend together both amplitude and phase angle dynamics. In [21], a Taylor Extended Kalman filter (TEKF) is introduced, separating the Taylor expansions of amplitude and phase angle. Different expansion orders can thus be applied to amplitude and phase, while harmonic frequencies can be tied to the fundamental.

The three-phase symmetry of typical power systems waveforms has been exploited in the literature to improve synchrophasor estimation (see [12] and [22] for a SV-based approach). In [23] the TEKF is generalized and applied to three-phase quantities. A unique model is used to include the three-phase parameters of the fundamental and harmonic components, while keeping into account the mutual relationships between phase angle evolutions. In particular, the frequency and its derivatives are unique, thus reflecting the physical properties of three-phase systems.

In this paper, which represents the extension of the research activity presented in [23], the definition of the process noise covariance matrix in the three-phase TEKF (3ph-TEKF) is deeply discussed. The description of the uncertainty associated with the equations describing the state evolution is crucial for the performance that the estimator can achieve under realistic conditions. A new approach is proposed in this paper: the uncertainty of the state transition is computed starting from a representation in the symmetrical components. This allows taking into account the *a priori* assumption that the measured three-phase quantity is almost symmetrical, as typically happens in a real-world scenario.

The paper shows, in particular, the advantages of such a solution for the estimation of the three-phases synchrophasors. Performance is assessed by simulations of complex conditions that combine different test signals from [2], [4], [24] also including three-phase unbalance [25] in order to stress dynamic tracking and disturbance rejection capabilities of the algorithm.

II. Three-Phase Taylor Extended Kalman Filter Synchrophasor Estimator

The implementation of a Kalman filter-based algorithm allowing synchrophasor and frequency estimation from measurement data basically requires that three relationships are available:

1) a dynamical system describing the time evolution of the state variables;
2) an algebraic equation that allows obtaining synchrophasor and frequency from the state variables;
3) an algebraic equation mapping the states to the measurment data.

Let us consider a three-phase system characterized by the rated frequency f_0 (corresponding to the angular frequency ω_0). We start by choosing an expression for the measurement data (measured signal); considering the pth phase ($p \in \{a, b, c\}$) it is:

$$s_p(t) = \Re\left\{ a_{p,1}(t) e^{j[\omega_0 t + \varphi_{p,1}(t)]} + \sum_{h=2}^{M} a_{p,h}(t) e^{j[h\omega_0 t + \varphi_{p,h}(t)]} \right\} \quad (1)$$

where $a_{p,1}(t)$ and $\varphi_{p,1}(t)$ represent the amplitude and phase angle of the phase p fundamental synchrophasor, while $a_{p,h}(t)$ and $\varphi_{p,h}(t)$ ($h \in \{2, \ldots, M\}$) denote the amplitude and phase angle of the hth order harmonic synchrophasor for phase p. These quantities are assumed to be slowly varying with respect to the f_0.

Now, an expression modeling the time evolution of the synchrophasors appearing in the output equation (1) has to be introduced. For this purpose, let us consider the following quantities as state variables (time dependency is not explicitly shown for the sake of brevity):

1) the fundamental angular frequency derivatives $\omega^{(k)}$, which are supposed to be also the phase-angle derivatives of order $k+1$ for the fundamental component of each system phase, up to the order N_ω, defining the vector $\mathbf{x}_\omega$ (symbol $'\top'$ indicates the transpose operator):
$$\mathbf{x}_\omega = \begin{bmatrix} \omega^{(0)} & \omega^{(1)} & \cdots & \omega^{(N_\omega)} \end{bmatrix}^\top \quad (2)$$
2) the phase p fundamental component amplitude derivatives $a_{p,1}^{(k)}$ up to the order N_1 and its phase angle $\varphi_{p,1}$, which are the elements of $\mathbf{x}_{p,1}$:
$$\mathbf{x}_{p,1} = \begin{bmatrix} a_{p,1}^{(0)} & a_{p,1}^{(1)} & \cdots & a_{p,1}^{(N_1)} & \varphi_{p,1} \end{bmatrix}^\top \quad (3)$$
Vector $\mathbf{x}_1$ is constructed by considering all the three phases as follows:
$$\mathbf{x}_1 = \begin{bmatrix} \mathbf{x}_{a,1}^\top & \mathbf{x}_{b,1}^\top & \mathbf{x}_{c,1}^\top \end{bmatrix}^\top \quad (4)$$
3) for each generic hth order harmonic, the phase p amplitude $a_{p,h}$ and phase angle $\varphi_{p,h}$, representing the components of the vector $\mathbf{x}_{p,h}$.
$$\mathbf{x}_{p,h} = \begin{bmatrix} a_{p,h} & \varphi_{p,h} \end{bmatrix}^\top \quad (5)$$
Vector $\mathbf{x}_h$ containing harmonic amplitudes and phase angles of all the phases is introduced:
$$\mathbf{x}_h = \begin{bmatrix} \mathbf{x}_{a,h}^\top & \mathbf{x}_{b,h}^\top & \mathbf{x}_{c,h}^\top \end{bmatrix}^\top \quad (6)$$

It is worth highlighting that a unique frequency (and its derivatives) has been defined in the model. This means that the evolutions of both fundamental and harmonic phase angles for all the three phases are assumed to be tied together. Furthermore, harmonic amplitude derivatives have not been included as state variables: since harmonics have typically much smaller magnitudes with respect to the fundamental, it is not needed to have a detailed representation of their dynamics. A noticeable reduction of model complexity is achieved under these assumptions.

Having defined the state variables, the state vector $\mathbf{x}$ is obtained by concatenating the previously defined vectors:

$$\mathbf{x} = \begin{bmatrix} \mathbf{x}_\omega^\top & \mathbf{x}_1^\top & \mathbf{x}_2^\top & \cdots & \mathbf{x}_M^\top \end{bmatrix}^\top \quad (7)$$

It turns out that its overall length is $N = N_\omega + 1 + 3(N_1 + 2M)$.

Now, the dynamical system ruling the time evolution of the state variables has to be defined. The state-space representation of the adopted model is linear and autonomous, thus:

$$\frac{d\mathbf{x}}{dt} = \mathbf{A}_c\mathbf{x} \tag{8}$$

Its behavior depends on the matrix $\mathbf{A}_c$, which can be partitioned as follows:

$$\frac{d}{dt}\begin{bmatrix}\mathbf{x}_\omega\\ \mathbf{x}_1\\ \mathbf{x}_2\\ \vdots\\ \mathbf{x}_M\end{bmatrix} = \begin{bmatrix}\mathbf{A}_\omega & \mathbf{0} & \mathbf{0} & \cdots & \mathbf{0}\\ \mathbf{A}_{1,\omega} & \mathbf{A}_1 & \mathbf{0} & \cdots & \mathbf{0}\\ \mathbf{A}_{2,\omega} & \mathbf{0} & \mathbf{A}_2 & \cdots & \mathbf{0}\\ \vdots & \vdots & \vdots & \ddots & \mathbf{0}\\ \mathbf{A}_{M,\omega} & \mathbf{0} & \mathbf{0} & \cdots & \mathbf{A}_M\end{bmatrix}\begin{bmatrix}\mathbf{x}_\omega\\ \mathbf{x}_1\\ \mathbf{x}_2\\ \vdots\\ \mathbf{x}_M\end{bmatrix} \tag{9}$$

Let us define the submatrices appearing in (9); it is straightforward to obtain that $\mathbf{A}_\omega$ is a $(N_\omega + 1) \times (N_\omega + 1)$ upper shift matrix. Reminding that the evolutions of the fundamental phase angles are assumed to be identical for the three system phases (because of the shared frequency), thus $\mathbf{A}_{1,\omega}$ is a $3(N_1 + 2) \times (N_\omega + 1)$ matrix defined as follows:

$$\mathbf{A}_{1,\omega} = \begin{bmatrix}\mathbf{0}_{(N_1+1)\times 1} & \mathbf{0}_{(N_1+1)\times N_\omega}\\ 1 & \mathbf{0}_{1\times N_\omega}\\ \mathbf{0}_{(N_1+1)\times 1} & \mathbf{0}_{(N_1+1)\times N_\omega}\\ 1 & \mathbf{0}_{1\times N_\omega}\\ \mathbf{0}_{(N_1+1)\times 1} & \mathbf{0}_{(N_1+1)\times N_\omega}\\ 1 & \mathbf{0}_{1\times N_\omega}\end{bmatrix} \tag{10}$$

Matrices $\mathbf{A}_{h,\omega}$ having size $6\times(N_\omega+1)$ are characterized by a similar structure, since the derivatives of the harmonic phase angles are supposed to be identical to that of the fundamental, but multiplied by the harmonic order h:

$$\mathbf{A}_{h,\omega} = \begin{bmatrix}0 & \mathbf{0}_{1\times N_\omega}\\ h & \mathbf{0}_{1\times N_\omega}\\ 0 & \mathbf{0}_{1\times N_\omega}\\ h & \mathbf{0}_{1\times N_\omega}\\ 0 & \mathbf{0}_{1\times N_\omega}\\ h & \mathbf{0}_{1\times N_\omega}\end{bmatrix} \tag{11}$$

Matrix $\mathbf{A}_1$ can be conveniently partitioned as:

$$\mathbf{A}_1 = \begin{bmatrix}\mathbf{A}_a & \mathbf{0} & \mathbf{0} & \mathbf{0} & \mathbf{0} & \mathbf{0}\\ \mathbf{0} & 0 & \mathbf{0} & 0 & \mathbf{0} & 0\\ \mathbf{0} & \mathbf{0} & \mathbf{A}_a & \mathbf{0} & \mathbf{0} & \mathbf{0}\\ \mathbf{0} & 0 & \mathbf{0} & 0 & \mathbf{0} & 0\\ \mathbf{0} & \mathbf{0} & \mathbf{0} & \mathbf{0} & \mathbf{A}_a & \mathbf{0}\\ \mathbf{0} & 0 & \mathbf{0} & 0 & \mathbf{0} & 0\end{bmatrix} \tag{12}$$

$\mathbf{A}_a$ is a $(N_1 + 1) \times (N_1 + 1)$ upper shift matrix, while $\mathbf{A}_h$, with $h > 1$, is a 2×2 null matrix.

It is useful to adopt the matrix notation also to express the three single-phase output equations (1). The vector of the three-phase measurement input $\mathbf{s}(t)$ is introduced, as well as the nonlinear time-varying vector of output functions $\mathbf{c}(\mathbf{x}, t)$:

$$\mathbf{s}(t) = \begin{bmatrix}s_a(t)\\ s_b(t)\\ s_c(t)\end{bmatrix} = \mathbf{c}(\mathbf{x}, t) \tag{13}$$

The previous equations are defined in the continuous time domain; therefore, they cannot be straightforwardly employed, since measurement data is obtained by sampling and execution is performed considering a time step T_s, supposed to be equal to the sampling time. The discrete time domain representation of (13) can be easily obtained by evaluating it in discrete time steps $t = kT_s$. Conversely, the continuous time state-space system (8) can be discretized obtaining the following representation:

$$\mathbf{x}(k + 1) = \mathbf{A}\mathbf{x}(k) \tag{14}$$

The discretized state-space matrix $\mathbf{A}$ can be obtained from $\mathbf{A}_c$ by using the expression:

$$\mathbf{A} = e^{\mathbf{A}_c T_s} \tag{15}$$

At $t = kT_s$, (14) allows obtaining a prediction of the state $\mathbf{x}^F(k+1)$ in the next time instant $(k+1)T_s$. Matrix $\mathbf{A}$ includes blocks related to magnitudes and phase angles of both fundamental and harmonic components. Focusing, for example, on the diagonal blocks associated with the fundamental, they are upper triangular and the kth diagonal is composed by elements equal to $T_s^k/k!$ thus linking the state forecast to a truncated Taylor expansion involving the derivatives included in the state; its order depends on the numbers of derivatives which have been considered in the continuous time representation.

Let us suppose that approximated dynamic modeling of the state variables results in an equivalent zero-mean process noise having covariance matrix $\mathbf{Q}$, thus reflecting the uncertainty in the state transition model. Under this assumption, the uncertainty of the state forecast is characterized by a covariance matrix $\mathbf{P}^F(k + 1)$ given by:

$$\mathbf{P}^F(k + 1) = \mathbf{A}\mathbf{P}(k)\mathbf{A}^\top + \mathbf{Q} \tag{16}$$

with $\mathbf{P}(k)$ the previous estimation covariance matrix.

Assuming that the measurement vector $\mathbf{s}$ is corrupted by zero mean noise characterized by a known covariance matrix $\mathbf{R}$, linearizing the output equation (13) with respect to the state vector $\mathbf{x}$ allows computing the minimum mean square error estimate of the state variables, which is provided by the following equation:

$$\begin{aligned}\mathbf{x}(k + 1) = \mathbf{x}^F(k + 1)+\\ + \mathbf{K}(k + 1)[\mathbf{s} - \mathbf{c}(\mathbf{x}^F(k + 1), (k + 1)T_s)]\end{aligned} \tag{17}$$

Kalman matrix gain $\mathbf{K}(k + 1)$ is obtained by computing:

$$\begin{aligned}\mathbf{K}(k + 1) \quad = \quad & \mathbf{P}^F(k + 1)\mathbf{C}^\top(k + 1)\\ & [\mathbf{C}(k + 1)\mathbf{P}^F(k + 1)\mathbf{C}^\top(k + 1) + \mathbf{R}]^{-1}\end{aligned} \tag{18}$$

Where $\mathbf{C}(k+1)$ is the Jacobian of the vector function $\mathbf{c}(\mathbf{x}, t$ evaluated in the point $(\mathbf{x}^F(k + 1), (k + 1)T_s)$, namely:

$$\mathbf{C}(k + 1) = \left.\frac{d\mathbf{c}(\mathbf{x}, t)}{d\mathbf{x}^\top}\right|_{\substack{\mathbf{x}=\mathbf{x}^F(k+1)\\ t=(k+1)T_s}} \tag{19}$$

The covariance matrix of the new estimated state is obtained as follows:

$$\mathbf{P}(k + 1) = (\mathbf{I} - \mathbf{K}(k + 1)\mathbf{C}(k + 1))\mathbf{P}^F(k + 1) \tag{20}$$

III. Obtaining Measurement and Process Noise Covariance Matrices

The behavior of the Kalman filter implementation strictly depends on the choice of the previously defined covariance matrices $\mathbf{Q}$ and $\mathbf{R}$ that define process and measurement noise, respectively. In particular, they appear in the expression (18) that allows computing the Kalman gain. Obtained estimates are as close to the optimal ones as much as these noises are able to represent the actual measurement and model uncertainties.

Let us start with measurements, which are assumed to be affected by the intrinsic errors occurring in the measurement process, other than noise and disturbances. These effects on the three phases are supposed to be modeled by independent and identically distributed random variables. Therefore, matrix $\mathbf{R}$ can be written as:

$$\mathbf{R} = \sigma_R^2 \begin{bmatrix} 1 & 0 & 0 \\ 0 & 1 & 0 \\ 0 & 0 & 1 \end{bmatrix} \tag{21}$$

Under this assumption, only the standard deviation σ_R has to be selected according to *a priori* knowledge.

Things become considerably trickier when the process noise covariance matrix $\mathbf{Q}$ has to be chosen. For the purpose, it can be partitioned as:

$$\mathbf{Q} = \begin{bmatrix} \mathbf{Q}_{\omega} & \mathbf{Q}_{1,\omega}^{\top} & \mathbf{Q}_{\mathbf{h},\omega}^{\top} \\ \mathbf{Q}_{1,\omega} & \mathbf{Q}_{1} & \mathbf{Q}_{\mathbf{h},1}^{\top} \\ \mathbf{Q}_{\mathbf{h},\omega} & \mathbf{Q}_{\mathbf{h},1} & \mathbf{Q}_{\mathbf{h}} \end{bmatrix} \tag{22}$$

where $\mathbf{Q}_{\omega}$ is the covariance matrix of the angular frequency and its derivatives, $\mathbf{Q}_1$ is that of the fundamental amplitude derivatives and phase angles, $\mathbf{Q}_{\mathbf{h}}$ takes into account harmonic amplitudes and phase angles. $\mathbf{Q}_{1,\omega}$ allows considering correlation between the fundamental component phase angles and amplitude derivatives and angular frequency derivatives. $\mathbf{Q}_{\mathbf{h},\omega}$ takes into account correlation between harmonics and angular frequency derivatives while $\mathbf{Q}_{\mathbf{h},1}$ includes the covariances between harmonics and fundamental. The major uncertainty source of the state forecast is represented by the finite number of magnitudes and phase angle derivatives that have been included in the state-space of the dynamical model. As previously stated, this results in truncated Taylor expansions of magnitudes and phase angles in the sampling instant as far as the discrete-time representation is concerned. A first possibility is to directly reason in terms of state variables, namely performing assumptions about the neglected *per phase* magnitudes and phase angles derivatives such as in [23].

A powerful alternative is decomposing the fundamental into its symmetrical components that allow favorably exploiting the characteristics of three-phase systems. The positive sequence component is typically the largest one by far, while negative and zero sequence terms have significantly smaller amplitudes. For this purpose, let us introduce $a_{+,1}(t)$ and $\varphi_{+,1}(t)$ as the magnitude and phase angle of the positive sequence dynamic phasor, $a_{-,1}(t)$ and $\varphi_{-,1}(t)$ those corresponding to the negative sequence dynamic phasor while $a_{0,1}(t)$ and $\varphi_{0,1}(t)$ are the amplitude and phase of the zero sequence dynamic component. Angular frequency and its derivatives are assumed to be shared by all the symmetrical components, just as in *per phase* quantities. Using the unitary formulation of the Fortescue transformation[1], the relationship between phase a, b and c fundamental dynamic phasors and the corresponding dynamic symmetrical components can be written; it results:

$$\begin{aligned} a_{p,1}(t)e^{j\varphi_{p,1}(t)} = \; & \tfrac{1}{\sqrt{3}} \Big[a_{+,1}(t)e^{j\left(\varphi_{+,1}(t) - r\frac{2\pi}{3}\right)} \\ & + \; a_{-,1}(t)e^{j\left(\varphi_{-,1}(t) + r\frac{2\pi}{3}\right)} \\ & + \; a_{0,1}(t)e^{j\varphi_{0,1}(t)} \Big] \end{aligned} \tag{23}$$

where $r = 0, 1, 2$ for phase a, b and c, respectively. By performing some computations on the previous expression, it is possible to obtain the state variables characterizing the fundamental component (namely the amplitude derivatives of the three phases $a_{p,1}^{(k)}$ up to the order $k = N_1$ and the three phase angles $\varphi_{p,1}$) as functions of the amplitude derivatives of the symmetrical components (namely $a_{+,1}^{(k)}$, $a_{-,1}^{(k)}$, $a_{0,1}^{(k)}$ up to the order $k = N_1$) and of the phase angles ($\varphi_{+,1}$, $\varphi_{-,1}$ and $\varphi_{0,1}$). It is clear that the prevailing positive sequence term generates strong correlation between phase quantities. Furthermore, the dynamic behavior can be assumed to be mostly driven by the positive sequence component; instead, the amplitude derivatives of the negative and zero sequence terms can be neglected. Under this assumption, it is possible to write the covariance matrix $\mathbf{Q}_{s,1}$ of the fundamental in terms of symmetrical components and then obtaining submatrix $\mathbf{Q}_1$ by using the Jacobian $\mathbf{J}$ of the relationship between state variables and their symmetrical components.

The first step is introducing some hypotheses that allow writing the covariance matrix $\mathbf{Q}_{s,1}$. For this purpose, it is reasonable to consider the positive sequence amplitude and phase modulated test signals defined by the synchrophasor standard [4] as representative of the typical dynamics that may occur in power systems. The expressions of the corresponding positive sequence synchrophasor magnitude and phase angle are:

$$\begin{aligned} a_{+}(t) &= \sqrt{6}S[1 + k_x \cos(\omega_m t)] \\ \varphi_{+}(t) &= k_a \cos(\omega_m t - \pi) \end{aligned} \tag{24}$$

where S is the RMS amplitude of the unmodulated single-phase signal, while ω_m and k_x are, respectively, the angular frequency and the relative amplitude of the modulating signal.

It should be noticed that the maximum value of the kth order magnitude derivative results:

$$a_{+,1,max}^{(k)} = \sqrt{6}Sk_x\omega_m^k \tag{25}$$

The model allows considering the derivatives of the positive sequence component up to order N_1. Since $1/f_m = 2\pi/\omega_m >> T_s$, the magnitude derivatives due to modulation can be assumed as constant during T_s. Therefore, supposing that the model starts from error-free state variables, the maximum forecast error of the kth order derivative can be obtained by a $(N_1 + 1 - k)$-fold time integration of the maximum value

[1] the inverse of the transformation matrix is equal to its conjugate transpose.

of the (N_1+1)-th derivative over the sampling interval:

$$e_{a_{+,1}^{(k)}} = \sqrt{6} S k_x \omega_m^{N_1+1} \frac{T_s^{N_1+1-k}}{(N_1+1-k)!} \tag{26}$$

Assuming a shape for the probability density function, the standard deviation $\sigma_{a_{+,1}^{(k)}}$ can be obtained from the corresponding maximum error:

$$\sigma_{a_{+,1}^{(k)}} = \frac{e_{a_{+,1}^{(k)}}}{k_c} \tag{27}$$

where k_c is a factor which is selected by assigning a confidence level to the maximum error. Covariances between amplitude derivatives are obtained by assuming full correlation.

The variances and covariances characterizing the zero and negative sequence component can be obtained in a similar fashion. Since a zeroth order expansion is used in this case, it is necessary to assume a maximum value for their derivatives. The corresponding maximum errors during the sampling interval can be computed by integration, while the standard deviations are obtained by guessing the shape of the probability density functions. Their dynamics are assumed to be independent, so covariances are supposed to be zero.

In order to define the standard deviations for the phase angles $\varphi_{+,1}$, $\varphi_{-,1}$ and $\varphi_{0,1}$ and their derivatives (shared by all of them and including the angular frequency) it is possible to adopt a similar approach. The dynamics of the angular frequency which occur during the phase modulation tests prescribed by [4] have to be considered in this case. Full correlation between phase angle derivatives is supposed.

Now all the elements that allow writing $\mathbf{Q}_\omega$ have been obtained. $\mathbf{Q}_{1,\omega}$ is completely defined since angular frequency and its derivatives are the same in the symmetrical components and in the phase quantities; zero correlation between angular frequency derivatives and magnitude derivatives is considered. Furthermore the $(6+N_1)\times(6+N_1)$ covariance matrix $\mathbf{Q}_{s,1}$ of the fundamental term in the symmetrical components can be obtained while, as aforementioned, $\mathbf{Q}_1$ is computed by using a proper Jacobian matrix $\mathbf{J}$. Furhter details are reported in Appendix A.

$\mathbf{Q_h}$ contains the variances and covariances of the harmonic amplitudes and phase angles. Variances of harmonic amplitudes can be obtained with the usual approach starting from a maximum value for their derivatives. Amplitudes of the different harmonics and phases are supposed to be uncorrelated. Zero correlation between amplitudes and harmonic phases is also assumed. Since angular frequency is unique, standard deviations of the harmonic phases are equal to that previously computed for the fundamental, but multiplied by the harmonic order h. This results in unitary correlations between phase angles of different harmonics and phases. Under the aforementioned assumptions, $\mathbf{Q}_{\mathbf{h},\omega}$ and $\mathbf{Q}_{\mathbf{h},1}$ are completely defined.

IV. Tests and Results

A. Test Assumptions

The proposed 3ph-TEKF estimation algorithm has been implemented in Matlab using 1 kHz sampling rate. The following assumptions have been introduced in order to compute the covariance matrices $\mathbf{Q}$ and $\mathbf{R}$:

- Second order expansion for the fundamental amplitude ($N_1 = 2$) and first order expansion for the angular frequency ($N_\omega = 1$) have been employed.
- Measurement noise standard deviation $\sigma_R = 3 \cdot 10^{-3}$ p.u. has been considered.
- Modulation angular frequency $\omega_m = 2\pi 5$ rad/s and modulation depths $k_x = 0.1$ and $k_a = 0.1$ rad for computing the maximum errors have been chosen as the most severe values reported in the synchrophasor standard.
- Maximum variation of the harmonic magnitudes within a sampling interval is assumed to be 10^{-4} p.u..
- Standard deviations have been obtained from the maximum errors by using $k_c = \sqrt{3}$.
- Negative and zero sequence components are assumed to be 1% of the positive one when computing the Jacobian.
- Harmonics up to order $M = 9$ have been included into the model.

The performance of the estimation algorithm has been assessed under different conditions, defined by combined tests that include different excitation signals chosen among those suggested in the standard [4] and in the guide IEEE C37.242 [24]. For some of the test signals, an additive white uniform noise, at a signal-to-noise ratio (SNR) of 70 dB, has been superimposed to stress the algorithms.

While in [23] positive sequence synchrophasor estimations were considered, in the following synchrophasor measurements for all the system phases are considered alongwith frequency measurements.

The performance indices are the usual Total Vector Error (TVE), which indicates the relative value of the vector error magnitude, absolute frequency error (|FE|), along with absolute amplitude error (|AE|) and phase angle error (|PE|).

All the test scenarios which are considered in the following except for the last one (Section IV-E) and for the noise contribution employ a symmetrical signal.

In the following, a comparison between the algorithm in [23], where the amplitude dynamics of the system phases were considered as uncorrelated in the definition of $\mathbf{Q}$, and the TEKF algorithm proposed in this paper, which uses a process noise covariance matrix defined starting from the symmetrical components, is carried out. The aim is to show the advantages obtained with more realistic assumptions about model uncertainty.

All the tests are performed with a duration of 10 seconds and a new measurement set is computed in each sampling interval.

B. Off-Nominal Frequency Tests

As a first test scenario, a purely sinusoidal 50 Hz signal of 1 p.u. amplitude is considered, with and without additive noise. Errors are negligible in the first case and thus the results reported in the following are only those achieved in the presence of superimposed noise; they mainly reflect the noise bandwidth of the two 3ph-TEKF implementations for the monitored quantities. Figs. 1 and 2 show phase a percent

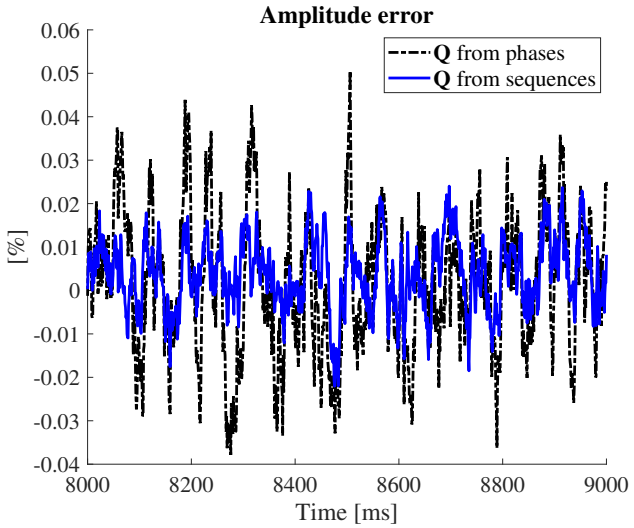

Fig. 1. Phase a TVE % under nominal frequency conditions, 70 dB SNR.

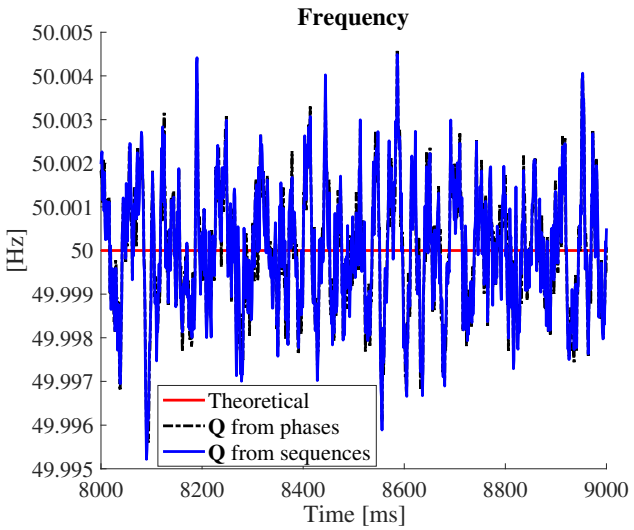

Fig. 2. FE under nominal frequency conditions, 70 dB SNR.

TVE and frequency estimation, respectively, for a 1-s portion of the considered signals (the time window shows steady-state conditions after initial transients have settled). Similar results can be found for the TVE of the other phases and thus they are not reported. Frequency measurements show only a slight difference between the methods (the root mean square of FEs is 5 mHz for both algorithms) while TVE is clearly lower when the new process noise covariance matrix is considered. In fact, the RMS TVE drops from $0.018\,\%$ to $0.014\,\%$ corresponding to an error reduction of about $26\,\%$. This difference is mainly due to the smaller AE and it reflects the importance of properly considering the link among the uncertainties of the phasor amplitudes of the different phases. This choice allows considerably reducing the infiltration of unwanted noise in the corresponding state variables.

Off-nominal frequency conditions have been simulated. Different tests have been performed considering the fundamental frequency range limits in [4]. In particular, the tests with $f = 45$ Hz and $f = 55$ Hz confirm the good frequency tracking capability of the filter. Errors are almost the same as those obtained under nominal frequency for the two methods, thus confirming that the main contribution comes from noise and that redefining $\mathbf{Q}$ in order to include correlation among phase quantities allows reducing TVE errors.

C. Harmonic Disturbance Tests

A second set of tests has been performed by superimposing three harmonics to the fundamental component. In particular, harmonic orders 3, 5, and 7 have been considered (which are among the most relevant ones in real-world scenarios). Magnitude is $5\,\%$ of the fundamental for all the harmonic orders (random initial phase angles are considered); tests at nominal and off-nominal frequencies (49 and 51 Hz) have been performed.

Only slight differences in the dynamics of the two methods with different $\mathbf{Q}$ matrices can be noticed, but the 3ph-TEKF shows remarkable harmonic rejection. Without additive noise TVEs are below TVE $= 0.03\,\%$, while including noise the results are very similar to those under off-nominal frequency reported in Section IV-B. The presence of the harmonics in the model proves to be thus very helpful in reducing their impact on the measurements for the fundamental components.

D. Modulation Tests

Since the focus of the proposed method is on dynamic conditions, modulation tests have been considered as representative of the variations that electrical signals may undergo. In particular, sinusoidal amplitude and phase-angle modulations are adopted (referred to as AM and PM in the following), using the signals defined by [4]. Frequency modulation $f_m \in (0, 5]$ Hz with modulation indices $k_x = 0.1$ and $k_a = 0.1$ rad, respectively for AM and PM, are used. In the following, results for $f_m = 5$ Hz under AM are discussed.

Both methods track the modulated amplitude of the signals, but Fig. 3 shows in detail the synchrophasor amplitude estimation error for phase a. It is clear that the new solution for defining $\mathbf{Q}$ clearly improves the accuracy, by significantly reducing the ripple in the estimates. The TVE is mainly affected by these AEs, since PE values are below 0.002 crad, and thus the TVE is reduced from $0.98\,\%$ to $0.77\,\%$.

It is interesting to notice that also frequency measurements benefit from the improved covariance matrix. FE values are reduced of about $43\,\%$ (from 19 mHz to 11 mHz).

Synchrophasor estimates for each phase under PM ($f_m = 5$ Hz) show a TVE reduction (see Fig. 4) of more than $6\,\%$ with the improved uncertainty description. This is due to a small reduction (about $4\,\%$) of the PEs, which is the most relevant in this scenario, and to a very strong reduction of AE, which becomes almost negligible.

The results of |FE| values are reported in Fig. 5 and they are below 97 mHz. The oscillatory behaviour of the error is strictly related to the approximated modeling of phase-angle dynamics, which is not able to consider all the derivatives.

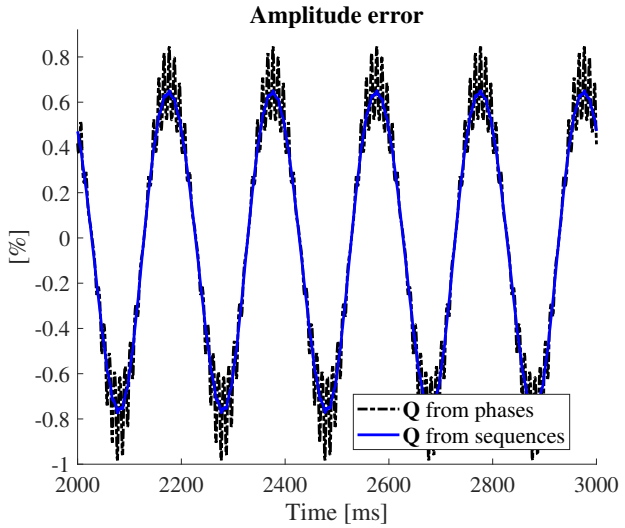

Fig. 3. Phase a Amplitude error under AM conditions.

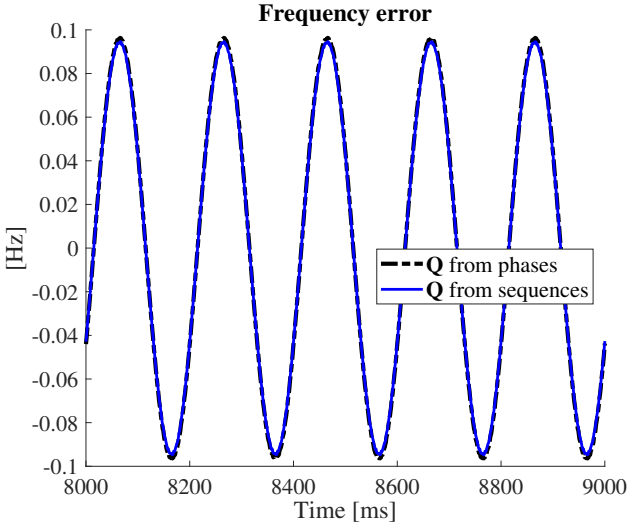

Fig. 5. FE under PM conditions.

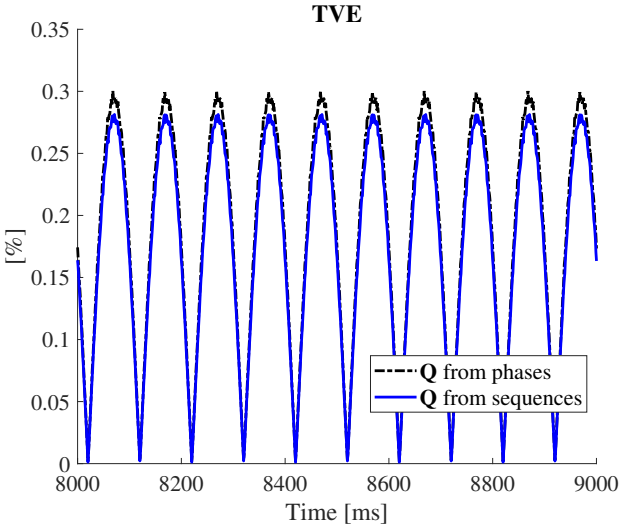

Fig. 4. Phase a TVE % under PM conditions.

E. Unbalance Tests

Three-phase systems and, in particular, distribution systems may suffer from a certain level of asymmetry between phases. For this reason, [24], for example, suggests to test instrumentation in the presence of unbalance. Therefore tests have been performed with both amplitude and phase-angle unbalance that are compatible with the assumptions reported above when **Q** has been computed. In particular, unbalance levels of $\pm 5\,\%$ and $\pm 10\,^\circ$ have been considered by changing either the amplitude or the phase angle of phase a at both $f = 50$ and $49\,\text{Hz}$. Tests have been also performed with or without additive noise. In all the performed tests, the effect of unbalance on the accuracy is negligible (TVE $< 10^{-2}\,\%$ and $|\text{FE}| < 0.1\,\text{mHz}$) with respect to the contribution due to additive noise because all the three-phases are included in the state vector (7). In the presence of noise, the advantages in terms of error reduction are similar to those observed in Section IV-B ($-26\,\%$ for TVE with phase unbalance equal to $+10\,^\circ$).

V. Conclusions

Synchrophasor and frequency measurement algorithms based on Kalman filtering have become popular in the last years. The main advantage is achieving very low latency, which represents an important feature for time-critical applications. In this work, a full three-phase Taylor Extended Kalman Filter synchrophasor estimator has been proposed. The introduced simplifications allow reducing the computational cost while obtaining remarkable dynamic behavior. Overall performance, in particular under amplitude modulation and in the presence of wideband noise, can be further improved by introducing a process noise covariance matrix which takes into account that in a real-world scenario, electrical quantities exhibit nearly three-phase symmetry. This can be performed by describing the model uncertainty in terms of symmetrical components; the method is particularly effective in improving the synchrophasor measurements of each phase. In addition, the proposed implementation also permits estimating harmonic components, which represents an important feature when it is employed in distribution grids.

Acknowledgements

Dr. Pegoraro work was partially funded by Fondazione di Sardegna for the research project "SUM2GRIDS, Solutions by mUltidisciplinary approach for intelligent Monitoring and Management of power distribution GRIDS".

Appendix A
Obtaining the Jacobian Matrix **J**

The Jacobian matrix **J** relating amplitude derivatives and phase angles of *per phase* synchrophasors and their symmetrical components counterparts can be obtained by properly manipulating (23). For this purpose, let us consider $N_1 = 2$. In this case, the expressions of phase a, b and c synchrophasor magnitude time derivatives up to the second order and of

those of the phase angles have to be computed. After that, the partial derivatives with respect to the magnitude time derivatives (from zeroth to second order) and to the phase angles of the symmetrical components have to be obtained; they represent the elements of the Jacobian. However, since the time derivatives of the zero and negative sequence term amplitudes are supposed to be negligible, $\mathbf{J}$ becomes a 12×8 matrix. Several terms contain trigonometric functions of differences between phase angles of different symmetrical components, or the magnitudes of the symmetrical components $a_{+,1}$, $a_{-,1}$ and $a_{0,1}$. This means that the Jacobian may change in each time step, and therefore it should be comtinuously updated and applied to $\mathbf{Q}_{s,1}$ in order to obtain $\mathbf{Q}_1$; however, this would result in a considerable computational burden. In order to reduce complexity, the expected value of the Jacobian is employed, having assumed that phase angles are independent and uniformly distributed in the interval $[-\pi, \pi]$ and having guessed values for the relative amplitudes of the negative and zero sequence components with respect to the positive sequence term. Further simplifications can be introduced by considering that negative and zero sequence terms are typically very small with respect to the positive sequence phasor. Finally, the nonzero terms of the Jacobian result:

$$\begin{array}{lll} \frac{\partial a_{p,1}^{(0)}}{\partial a_{+,1}^{(0)}} \simeq \frac{1}{\sqrt{3}} & \frac{\partial a_{p,1}^{(0)}}{\partial a_{-,1}^{(0)}} \simeq \frac{1}{\sqrt{3}} \frac{a_{-,1}}{a_{+,1}} & \frac{\partial a_{p,1}^{(0)}}{\partial a_{0,1}^{(0)}} \simeq \frac{1}{\sqrt{3}} \frac{a_{0,1}}{a_{+,1}} \\ \frac{\partial a_{p,1}^{(1)}}{\partial a_{+,1}^{(1)}} \simeq \frac{1}{\sqrt{3}} & \frac{\partial a_{p,1}^{(2)}}{\partial a_{+,1}^{(2)}} \simeq \frac{1}{\sqrt{3}} & \frac{\partial \varphi_{p,1}}{\partial \varphi_{+,1}} \simeq 1 \end{array} \tag{28}$$

REFERENCES

[1] AA. VV., *Phasor Measurement Units and Wide Area Monitoring Systems*, 1st ed., A. Monti, C. Muscas, and F. Ponci, Eds. Academic Press, 2016.

[2] *IEEE Standard for Synchrophasor Measurements for Power Systems*, IEEE IEEE Std C37.118.1-2011, Dec. 2011.

[3] *IEEE Standard for Synchrophasor Measurements for Power Systems – Amendment 1: Modification of Selected Performance Requirements*, IEEE IEEE Std C37.118.1a-2014, Apr. 2014.

[4] *IEEE/IEC International Standard - Measuring relays and protection equipment - Part 118-1: Synchrophasor for power systems - Measurements*, IEEE/IEC IEC/IEEE 60255-118-1:2018, Dec 2018.

[5] J. A. de la O Serna, "Dynamic phasor estimates for power system oscillations," *IEEE Trans. Instrum. Meas.*, vol. 56, no. 5, pp. 1648–1657, Oct. 2007.

[6] C. Huang, X. Xie, and H. Jiang, "Dynamic phasor estimation through DSTKF under transient conditions," *IEEE Trans. Instrum. Meas.*, vol. 66, no. 11, pp. 2929–2936, Nov 2017.

[7] W. Premerlani, B. Kasztenny, and M. Adamiak, "Development and implementation of a synchrophasor estimator capable of measurements under dynamic conditions," *IEEE Trans. Power Del.*, vol. 23, no. 1, pp. 109–123, Jan. 2008.

[8] R. K. Mai, Z. Y. He, L. Fu, B. Kirby, and Z. Q. Bo, "A dynamic synchrophasor estimation algorithm for online application," *IEEE Trans. Power Del.*, vol. 25, no. 2, pp. 570–578, Apr. 2010.

[9] G. Frigo, A. Derviskadic, and M. Paolone, "Reduced leakage synchrophasor estimation: Hilbert transform plus interpolated DFT," *IEEE Trans. Instrum. Meas.*, pp. 1–16, 2018.

[10] D. Petri, D. Fontanelli, and D. Macii, "A frequency-domain algorithm for dynamic synchrophasor and frequency estimation," *IEEE Trans. Instrum. Meas.*, vol. 63, no. 10, pp. 2330–2340, Oct. 2014.

[11] P. Castello, J. Liu, C. Muscas, P. A. Pegoraro, F. Ponci, and A. Monti, "A fast and accurate PMU algorithm for P+M class measurement of synchrophasor and frequency," *IEEE Trans. Instrum. Meas.*, vol. 63, no. 12, pp. 2837–2845, Dec. 2014.

[12] S. Toscani and C. Muscas, "A space vector based approach for synchrophasor measurement," in *IEEE I2MTC*, May 2014, pp. 257–261.

[13] P. Castello, R. Ferrero, P. A. Pegoraro, and S. Toscani, "Space vector Taylor-Fourier models for synchrophasor, frequency, and ROCOF measurements in three-phase systems," *IEEE Trans. Instrum. Meas.*, vol. 68, no. 5, pp. 1313–1321, May 2019.

[14] M. Bertocco, G. Frigo, C. Narduzzi, C. Muscas, and P. A. Pegoraro, "Compressive sensing of a Taylor-Fourier multifrequency model for synchrophasor estimation," *IEEE Trans. Instrum. Meas.*, vol. 64, no. 12, pp. 3274–3283, Dec 2015.

[15] I. Kamwa, S. R. Samantaray, and G. Joos, "Wide frequency range adaptive phasor and frequency pmu algorithms," *IEEE Trans. Smart Grid*, vol. 5, no. 2, pp. 569–579, Mar. 2014.

[16] J. A. de la O Serna and J. Rodriguez-Maldonado, "Instantaneous oscillating phasor estimates with Taylor-Kalman filters," *IEEE Trans. Power Syst.*, vol. 26, no. 4, pp. 2336–2344, Nov. 2011.

[17] J. Liu, F. Ni, J. Tang, F. Ponci, and A. Monti, "A modified Taylor-Kalman filter for instantaneous dynamic phasor estimation," in *IEEE PES Innovative Smart Grid Technologies (ISGT) Eur. Conf.*, 2012.

[18] D. Fontanelli, D. Macii, and D. Petri, "Dynamic synchrophasor estimation using smoothed Kalman filtering," in *IEEE I2MTC*, May 2016.

[19] J. de la O Serna and J. Rodriguez-Maldonado, "Taylor-Kalman-Fourier filters for instantaneous oscillating phasor and harmonic estimates," *IEEE Trans. Instrum. Meas.*, vol. 61, no. 4, pp. 941–951, Apr. 2012.

[20] J. Liu, F. Ni, P. A. Pegoraro, F. Ponci, A. Monti, and C. Muscas, "Fundamental and harmonic synchrophasors estimation using modified Taylor-Kalman filter," in *Proc. of IEEE AMPS*, Sep. 2012, pp. 1–6.

[21] R. Ferrero, P. A. Pegoraro, and S. Toscani, "Dynamic fundamental and harmonic synchrophasor estimation by extended kalman filter," in *Proc. of IEEE Appl. Meas. for Pow. Syst. (AMPS)*, Sep. 2016, pp. 1–6.

[22] S. Toscani, C. Muscas, and P. A. Pegoraro, "Design and performance prediction of space vector-based PMU algorithms," *IEEE Trans. Instrum. Meas.*, vol. 66, no. 3, pp. 394–404, Mar. 2017.

[23] R. Ferrero, P. A. Pegoraro, and S. Toscani, "Three-phase synchrophasor estimation through Taylor extended Kalman filter," in *2019 IEEE 10th International Workshop on Applied Measurements for Power Systems (AMPS)*, Sep. 2019, pp. 1–6.

[24] *IEEE Guide for Synchronization, Calibration, Testing, and Installation of PMUs for Power System Protection and Control*, IEEE IEEE C37.242-2013, Mar. 2013.

[25] P. Castello, R. Ferrero, P. A. Pegoraro, and S. Toscani, "Effect of unbalance on positive-sequence synchrophasor, frequency, and ROCOF estimations," *IEEE Trans. Instrum. Meas.*, vol. 67, no. 5, pp. 1036–1046, May 2018.

Roberto Ferrero (S'10-M'14-SM'18) is a Senior Lecturer (Associate Professor) with the Department of Electrical Engineering and Electronics, University of Liverpool, UK. His main research activity is focused on electrical measurements, particularly applied to power systems and electrochemical devices. He is a member of the IEEE Instrumentation and Measurement Society, and of its TC 39 (Measurements in Power Systems), and he is an Associate Editor of the IEEE Transactions on Instrumentation and Measurement.

Paolo Attilio Pegoraro (M'06-SM'19) is currently Associate Professor with the Department of Electrical and Electronic Engineering, University of Cagliari, Cagliari, Italy. He has authored or co-authored over 100 scientific papers. His research interests include the development of new measurement techniques for modern power networks. Dr. Pegoraro is a member of IEEE Instrumentation and Measurement Society TC 39 (Measurements in Power Systems) and of IEC TC 38 (Instrument Transformers) WG 47. He is an Associate Editor of the IEEE Transactions on Instrumentation and Measurement.

Sergio Toscani (S'08, M'12, SM'19) is Assistant Professor with the Dipartimento di Elettronica, Informazione e Bioingegneria, Politecnico di Milano. His research activity is mainly focused on development and testing of current and voltage transducers, measurement techniques for powers systems, electrical components and systems diagnostics. Dr. Sergio Toscani is member of the IEEE Instrumentation and Measurement Society and of the TC-39 - Measurements in Power Systems.